Investigation of two-phase bubbly flows using laser doppler anemometry

Jean-Louis Marié

PCH PhysicoChemical Hydrodynamics Vol. 4, No. 2, pp. 103–118, 1983.
Printed in Great Britain

0191–9059/83 $3.00 + 0.00

INVESTIGATION OF TWO-PHASE BUBBLY FLOWS USING LASER DOPPLER ANEMOMETRY

J. L. MARIÉ

Laboratoire de Mécanique des Fluides, Ecole Centrale de Lyon, BP 163 36, Avenue Guy de Collongue, 69130 Ecully, France

(*Received for publication* 1 *November* 1982)

Abstract—The present work is devoted to the development of an accurate and reliable laser Doppler anemometer technique (L.D.A.) meant for the measurement of the characteristics of two-phase bubbly flows. Most of these characteristics are the various statistical moments of the velocity fluctuations and the Reynolds stress tensor components within the continuous phase but also, under well defined conditions, the mean slip velocity of the dispersed phase. Although this technique was applied to a turbulent cocurrent vertical air–water bubbly flow in a large square channel (450 × 450 mm^2), it is believed that it can be extended to many other two-phase dispersed flow patterns, since a wide variety of experimental conditions was successfully explored: the mean liquid velocity and the local void fraction ranged respectively from 0 to 1.2 m/s and from 0 to 7%, while the mean bubble diameter was of the order of 5 mm. The technique employed is derived from the classical differential Doppler detection and forward diffusion method, which is adapted to the case of a bubbly flow by choosing the appropriate signal processing method. Comparison with results previously obtained in the same facility with a conical hot film anemometer clearly demonstrates the accuracy of the method within limits which are discussed.

1. INTRODUCTION

In recent years, many attempts have been made at extending the use of laser Doppler anemometry to particulate or bubbly flows. In their detailed theoretical analysis of the phenomena occurring when laser beams cross a bubble, Durst and Zare [1] have generalized the classical Doppler formula to the case of large bodies and proposed theoretical relations for the determination of interface velocities. On the other hand, from a more practical point of view, a number of experiments have been conducted in different flow patterns, using various optical and electronic set-ups [2]. Unfortunately as noted by Delhaye [3] and Hewitt [4], most of these experiments are far from being totally convincing: the dimensions of the test sections generally used are small (a few centimeters); very few physically relevant parameters are measured or if they are, no comparison with other metrologies is made, so that it is quite difficult to know whether the methods proposed are reliable.

The present paper is devoted to what is believed to be a thorough investigation of the real possibilities of the L.D.A. technique—i.e. its reliability, its advantages and limitations when studying two-phase dispersed flows. The experimental facility, the optical set-up and electronics are described in the next section which is followed by the presentation of the analysis of the Doppler signal and its processing. A critical evaluation of the method is then made and the paper ends with summary conclusions.

2. EXPERIMENTAL FACILITY, OPTICAL SET-UP AND ELECTRONICS

2.1. *Description of the experimental facility*

A hydrodynamic tunnel (see Fig. 1), described in detail in [5] delivers a uniform mean flow. The 2 m long square test section (450 × 450 mm^2) is operated at atmospheric pressure and

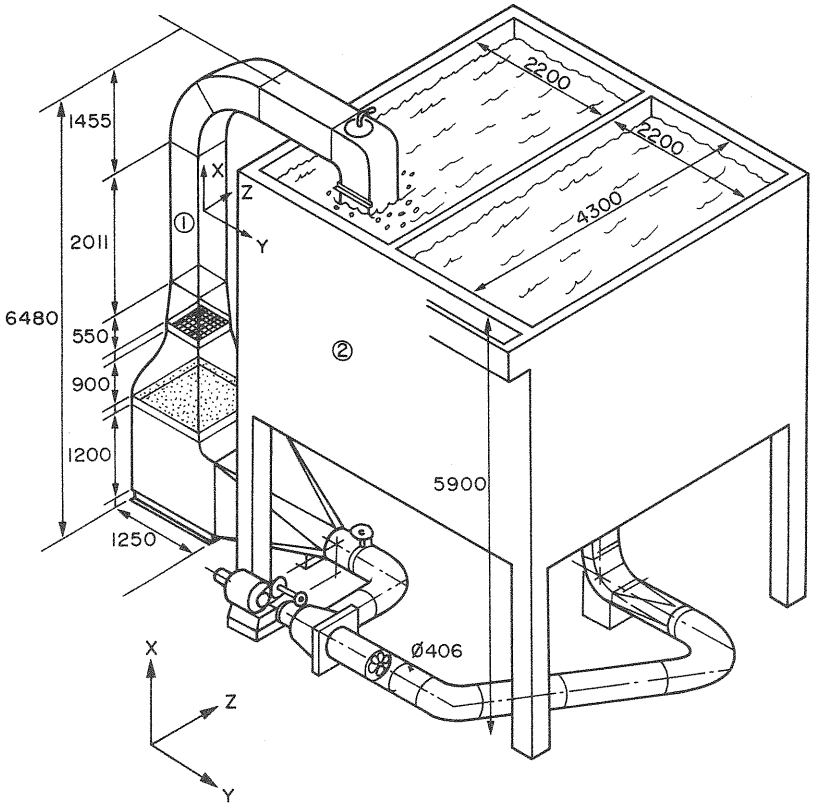

Fig. 1. General view of the facility and liquid coordinate system. 1. Test section; 2. Water tank.

ambient temperature, at mean liquid velocities as large as 1.2 m/s. A grid, located upstream and made of cylindrical rods, generates a homogeneous turbulent flow of water which is made isotropic, by a contraction section of ratio 1.27. The dimensions of the test section, of the grid mesh spacing (4 cm) and the diameter of the rods (8 mm) have been so chosen as to obtain turbulent length scales which are both large enough to be measured with the standard local probes and of the same order of magnitude as the diameter of the air bubbles. The physically relevant quantities which describe the above single phase turbulent flow and their values are the following: integral length scale, $l = 2$ cm; Kolmogorov's length scale, $\eta = 0.53$ mm; Reynolds number based on grid-mesh spacing, $R_m = \dfrac{UM}{\nu} = 10\,500$; turbulent Reynolds number, $u'\lambda/\nu = 35$; where ν, λ, U, u' and M stand respectively for the kinematic viscosity, Taylor's length scale, the longitudinal mean velocity, the r.m.s. value of the longitudinal velocity fluctuation u, and the grid-mesh spacing. The dispersed phase consists of a swarm of air bubbles which are blown uniformly into the tunnel through 260 equally spaced injectors, 0.8 mm in diameter and 30 mm long, distributed on the upper generating line of every rod parallel to the Y axis, with an alternate inclination of $\pm 15°$ on the vertical (see Fig. 2). Each rod is individually supplied with air, which makes it possible, if need be, to generate screens of bubbles in different regions of the test section. Under those conditions, the mean bubble diameter is about 5 mm and the void fraction varies from 0 to 10% according to the injection pressure.

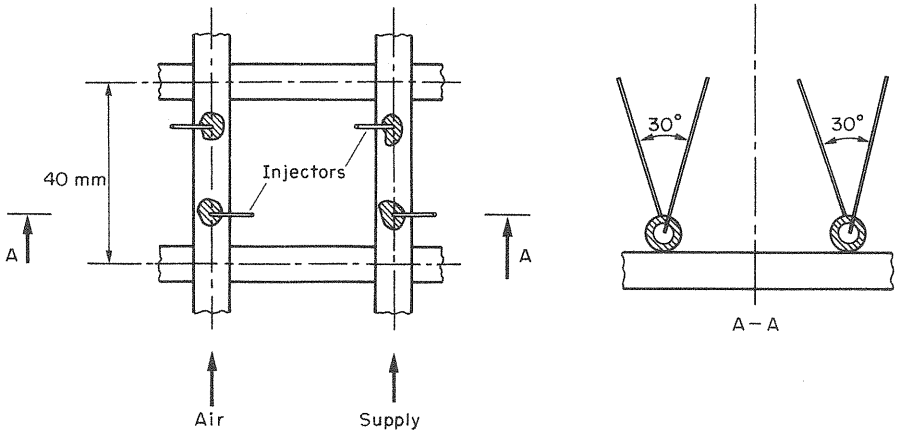

Fig. 2. Detail of the injection arrangement.

2.2. *The optical and electronic set-up*

The optical set-up selected is shown in Fig. 3. The emitting system is a 2.5 W Spectra Physics 164 A–Kr laser used in a single color mode with a wavelength of 514.5 mm. A 55 × 25 DISA separator splits the monochromatic light emitted into two parallel beams which are then focused on a given point of the test section by a 600 mm focal lens. Due to the fringe pattern thus created, any small contaminating particle moving through the control volume scatters light whose intensity is modulated with a frequency F_D which is proportional to the normal component U of the particle velocity. The latter may therefore be obtained from:

$$U = F_D i = F_D \frac{\lambda}{2 \sin \frac{\theta}{2}}$$

where θ is the angle formed by the laser beams, λ the wavelength of the laser beam in the medium surrounding the measuring volume and i the fringe spacing. As the beams intersect with a 5.8° angle in air, the control volume, 3 mm long and 0.2 mm in diameter, contains about 40 fringes, which is enough to obtain a good quality Doppler signal, especially a high ratio of validated particles. Furthermore since the fringe spacing is 5.150 μm, the frequencies to be processed range from 58 to 235 kHz, which fits quite satisfactorily with the possibilities of the DISA 55 L 90 counter employed here. The light scattered by the particles is collected by

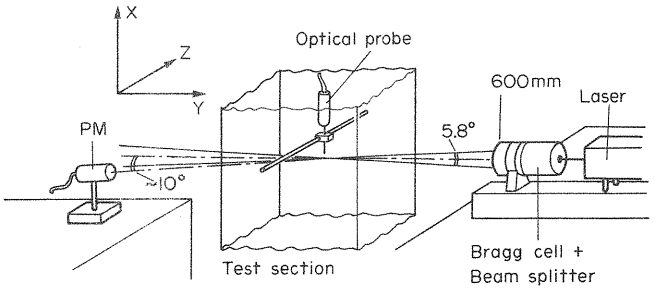

Fig. 3. Optical set-up.

a photomultiplier DISA 55 × 08 located nearly symmetrically with respect to the plane $y = 0$, 600 mm away from it. As noted by Boutier [6] or Durst, Melling and Whitelaw [7], this forward scattering arrangement is advantageous because it is easier to set-up than the reference beam mode and also because it provides a Doppler signal which has a good signal-to-noise ratio. Here, however, it was chosen for another reason. In fact, as in any particulate flow, it was noticed that the light intercepted by bubbles or contaminating particles was re-emitted forward with maximum intensity. Bearing in mind the remarks made by Martin *et al.* [8], a differential detection method therefore appeared to be particularly appropriate to the measurement of each phase velocity. The P.M. output is fed into a counter which is itself connected to a data processing computer. In essence, the latter consists of a Hewlett-Packard central unit of 32 kwords, a magnetic disk H.P. 7905 (permanent support: 5 M octets, removable support: 10 M octets) and a terminal control system Tektronix 4010. The computer can record the frequency data validated by the counter and process it instantaneously or later, with the Fortran programs already in use in the laboratory for this type of anemometry.

Practically, the preliminary tests made in single phase flow were satisfactory. The chemical analysis of the water flowing in the tunnel showed it to be hard water and its characteristics fortunately turn out to be most convenient for this type of anemometry. In fact, its concentration in solid particles is low enough to support the assumption of independent diffraction, but at the same time high enough for the light emitted by the control volume towards the observer to be intense. As a consequence, a large amplitude Doppler signal is obtained, whose quality only depends on the voltage supply of the P.M. If the latter is low, the number of validated particles is large and the signal to noise ratio is good, with a marked optimum however at about 1.2 kV. Above this value, the electronic noise of the counter, which is originally negligible is considerably amplified and its amplitude exceeds erratically the 200 mV level, thereby disturbing the counting of the relevant frequencies. In order to avoid this phenomenon, a common voltage supply of 1.2 kV, was chosen for the single phase experiments. Under such conditions, the longitudinal turbulent intensities measured at the center of the test section, agree within better than 5% with those obtained with a conical hot-film anemometer, thus justifying *a posteriori* the options made. Finally the use of a rotating beam splitter makes it possible to measure the cross turbulent intensities and Reynolds tensor components very simply, according to the method devised by Yanta and Smith [9] which consists of taking values of the turbulent intensity of 0° and $\pm 45°$ angles relative to the x direction.

3. SIGNAL ANALYSIS AND PROCESSING

3.1. *Signal analysis*

Up till now, most measurements using laser Doppler anemometry in two-phase dispersed flow, such as air–water bubbly flows, were performed in vertical test sections of small diameter. The swarm of bubbles or drops which are injected into the liquid remains therefore narrow and shuts out the laser beams only in the vicinity of the control volume. Distortions of the Doppler signal which are thus detected consist in large amplitude modulations whose frequency depend to a large extent on the mean velocity of the dispersed phase [1, 10]. Unfortunately such a statement does not apply to the present study since it takes no account of the noise generated by the interruption of the beams outside the control volume. If this fundamental phenomenon may well be neglected in the above-mentioned cases, it becomes important, here, when operating a facility whose test section is rather large (450×450 mm^2). As a consequence, the complete Doppler signal is actually composed of three contributions:

a Doppler frequency associated with the velocity of the liquid phase, another frequency which apparently may be connected to the rising velocity of the bubbles and also an important electronic noise due to the large refractive index gradients of the medium which is crossed. In order to better appraise these different components, the experiment sketched in Fig. 4 was considered. Screens of bubbles were generated successively in three different areas of the flow, whose location was of interest with regard to the measuring point and in each case the Doppler signal delivered by the P.M. was analyzed. As a rule, when the screens were formed in regions 1, 2 or 3, the number of validated particles decreased more or less sharply according to the air supply. This decrease is caused by the numerous interruptions of the beams which involve either the disappearance of the measuring point or the progressive reduction of the time of presence of the continuous phase at this point. Under those conditions, one may either retain the functioning conditions which prove successful in single phase flow even though it requires a very long measuring time or artificially increase the rate of validated information by using a higher voltage supply for the P.M. In what follows, both solutions are explored and their consequences on the Doppler signal characteristics are studied in detail, as well as the possible means of solving the various processing problems they raise.

When air is blown up into regions 1 or 2, the beams are interrupted only far from the point where they intersect. In this case the control volume vanishes, while the light absorbed by the gas is reflected by the surfaces of the numerous bubbles rising near the interruption point and is diffused in the whole forward space through a multitude of very short and high intensity flashes. Owing to the flash light, the impurities in the water which were confined in the vicinity of the measuring point just before it vanished are strongly lit up, which in some sense dazzles the sensitive part of the P.M. Inspection of the Doppler output of the counter reveals that this dazzle amplifies the noise of electronics in proportions which depend on the voltage supply used for the P.M. When this voltage supply is rather high, it is observed that some of the frequency components of this noise exceed the 200 mV high level of the counter, thereby causing the validation of irrelevant frequencies. The latter being diffuse over the whole range of frequencies to be processed, their suppression of the signal using the counter filters is impossible. This is the reason why the measurements made under such conditions are erroneous: in particular the longitudinal turbulent intensity values prove to be three or four times larger than what is normally expected in a region of the flow where no bubble is present. It is interesting however to note that the noise component due to optical phenomena is less important in 2 than in 1. As shown in Fig. 5, this can probably be attributed to the fact that the detector is located in a region where it is less affected by undesirable light than in 1; moreover the bubble screen shields the measuring point. The same remark applies to the case

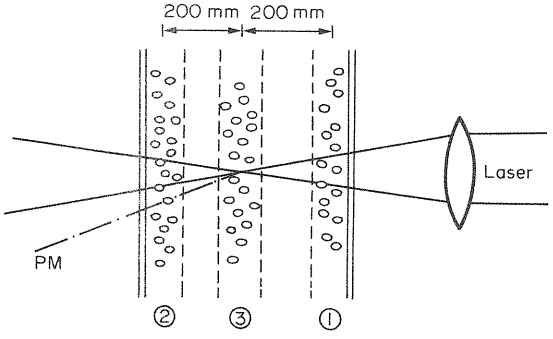

Fig. 4. Bubble screen experiment.

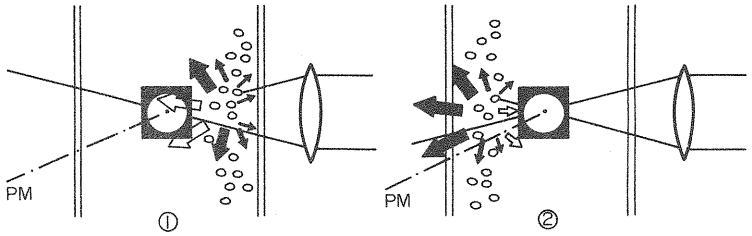

Fig. 5. Influence of the P.M. location on it sensitivity to the undesirable light.

when the air supply is limited to a narrow strip in the center of the test section. In the latter situation however, the amplification of the electronic noise is not the only consequence of the presence of the gas. Indeed, the Doppler signal also exhibits amplitude modulations which are associated with the bubbles flowing through the control volume. When looking at the analog output of the counter, we note that these modulations are linked to the velocity peaks of variable amplitude. Experiments made independently in a square tank (1 m × 1 m) filled with water into which single bubbles were injected provide us with more detailed quantitative information on this phenomenon. In agreement with Lee and Srinivasan [11], it is to be noticed that each of the observed peaks in fact corresponds to an amplitude modulation of the Doppler signal which is generated by scattering from either the forward or backward bubble interface which crossed the measuring volume. The characteristics of the interface modulations is that observed by Martin *et al.* [8] and since they thoroughly examined the various factors influencing them, it did not appear useful to go over their interpretation with which the author agrees. On the other hand it should be stressed at this point that when the control volume is within the air confined in a bubble the counter output exhibits no signal but an electronic noise whose level, as in the injection pattern 1 or 2, depends on the voltage supply of the P.M. If the latter is low, this level remains small and in this case the bubble signal is only constituted by the forward and backward interface signals. The velocity peaks which respectively correspond to these signals are approximately equal together and can be proved to be almost equal to the rising velocity of the bubbles (Fig. 7a) by making photographic measurements (Fig. 8). Following the theoretical formulation given by Durst and Zare, it is thus clear that the behaviour of such air ellipsoidal bubbles is the same as that of a spherical reflecting spheres whose radius would be equal to the curvature radius of their forward or backward interface (see Fig. 6). However, if the voltage supply is high, the noise level increasing beyond the 200 mV threshold, a sequence of irrelevant informations is then validated during the passage of the control volume within the bubble. As it can be seen on Fig. 7(b), it is no more possible to discriminate the interfaces peaks from

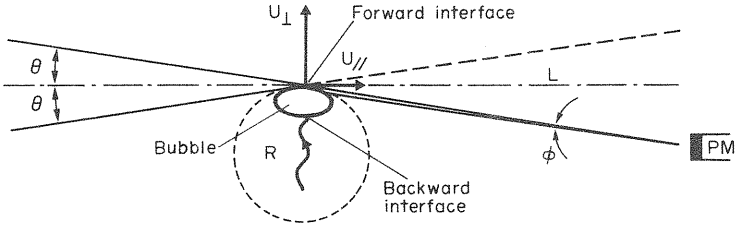

Fig. 6. Formulation of the Doppler effect for a reflecting spherical sphere according to Durst and Zare. Simplification in the case of large values of L/R, i.e. ϕ small.

$$F_D = 2(U_\perp \cos \phi \pm U_\parallel \sin \phi) \sin (\theta/\lambda) \rightarrow F_D = 2_\perp \sin (\theta/\lambda)$$

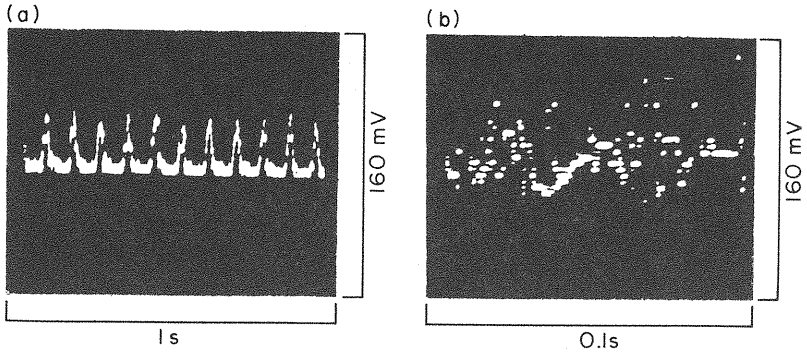

Fig. 7. Two examples of the analog signal of the counter when single bubbles pass successively through the measuring point. (a) Low P.M. voltage supply; velocity scale: 0.75 cms^{-1}/mV. $\bar{U}_B^x \simeq 27$ cm/s; bubble diameter: 4 mm. (b) High P.M. voltage supply; velocity scale: 0.75 cms^{-1}/mV. $\bar{U}_B^x$ undetermined.

the erroneous data: the bubble signal which in this case becomes uninteresting, must be suppressed from the complete Doppler signal.

In view of the above discussion we now understand better the possibilities offered by each functioning condition. It is obvious that any measurement of the rising velocity of the bubbles implies the selection of a low voltage supply. Then, for a standard measurement-time, the signal will contain very little information on the liquid phase and the level of the electronic noise will not be very important. It is the reason why in this case the velocity peaks generated by bubble interfaces can be well identified, easily discriminated from the mean analog signal (the slip velocity $\bar{U}_B^x - \bar{U}_L^x$ is not nil) and finally be used to measure the mean rising velocity of the bubbles. On the other hand, if the turbulence characteristics of the continuous phase are required, a higher voltage supply should be preferred since it provides a good quality signal in the liquid. The latter, however, has to be processed in three different steps which are listed below in chronological order:

(A) Elimination of undesirable electronic frequencies.
(B) Discrimination between the two different phases.
(C) Calculation of the turbulence parameters.

If very few authors seem to have considered the first problem some of them have addressed themselves to the problem of the discrimination between frequency components created by

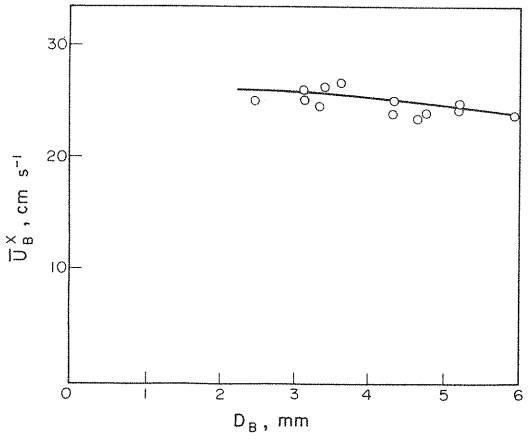

Fig. 8. Tank experiments: photographic measurements of the mean rising velocity of single bubbles.

each of the two phases. To this effect, Davies [12] and Sullivan [13] use a discrimination criterion based on the analysis of the signal amplitude whereas Durst [1] improves the method by using filter banks. However none of the foregoing solutions can be fully satisfactory as long as the above-mentioned chronology is not followed. This is precisely why we develop herein a method well adapted to our study and whose principle is believed to be applicable to any situation where the same kind of signal is found.

3.2. *Signal processing*

(a) *Elimination of undesirable electronic frequencies.* As emphasized in the previous paragraph, the elimination of the electronic noise is an essential step in the signal processing. But since this noise is diffuse over the whole range of frequencies to be processed whatever this range, its suppression from the signal is impossible when using filters or when trying to modify this range by choosing a new value of the fringe spacing. Therefore another system, described below, has to be selected to reach such a goal.

The corresponding set-up consists of a frequency-shifter DISA 55 N 90 and a Bragg cell which is directly connected to it and modulates one of the beams with its own frequency F_B thereby causing the motion of the fringes within the measuring volume. In our particular case, the fringes move in the same direction as the flow and thus the light emitted by a particle whose velocity corresponds to a frequency F_D, is detected by the P.M. with a frequency $F_{PM} = F_B - F_D$. As mentioned in Section 2.2, such a signal is then fed into the counter where it is validated if its amplitude and the number of its periods are sufficient. Since this happens at intervals varying with time, information at this level is composed of an almost random sample of frequencies of the two phases. In order to optimize the storage of these frequencies in computer memories, they are recorded on a disk one after the other without any time basis. As soon as this is done, a calculating program gives each recorded data its real frequency F_D and then transforms it into a velocity. The recombined signal constituted by all these velocities may be displayed on the terminal control system Tektronix. The efficiency of the method appears in the results obtained in situation 1 and 3 of the previous experiment. As a matter of fact, when using the Bragg cell, it is observed that the electronic noise of the liquid signal, which was originally diffuse is now centered around F_B. Consequently, each time the laser beams are interrupted elsewhere than in the control volume, the noise is amplified above the 200 mV level and validated by the counter as being a frequency $F_{PM} \sim F_B$. The latter being numerically calculated from $F_D = F_B - F_{PM}$, the disturbance due to these beams interruptions appears as shown in Fig. 9, namely as a sequence of zero velocity peaks which it is indispensable to get rid of. They appear in greater numbers in injection pattern 1 than in 2, which can be explained by the remarks already made in Section 3.1 on the sensitivity of the P.M. to undesirable light. Their elimination is achieved by an amplitude discrimination, when recording the data. In this purpose a low amplitude threshold must be inserted in the recording program.

Before discussing the second step of the processing, it is worthwhile noting that the use of a Bragg cell has at least two more advantages. Because it allows a high ratio of particle validation it enables to work with a lower voltage, which turns out to be particularly convenient when trying to measure the velocities of the bubbles. Furthermore, due to the frequency shifting, the origin of the frequencies to be processed can be translated and thus flows whose mean velocities are very low or even vanish may be investigated.

(b) *Discrimination between the two phases.* Figure 10 gives two examples of the signal obtained after the previous step, which illustrate the two possible modes of functioning. When using a low voltage supply of the P.M. (Fig. 10a), the velocity peaks created by interfaces passages can be well identified and there is no discrimination problem between the

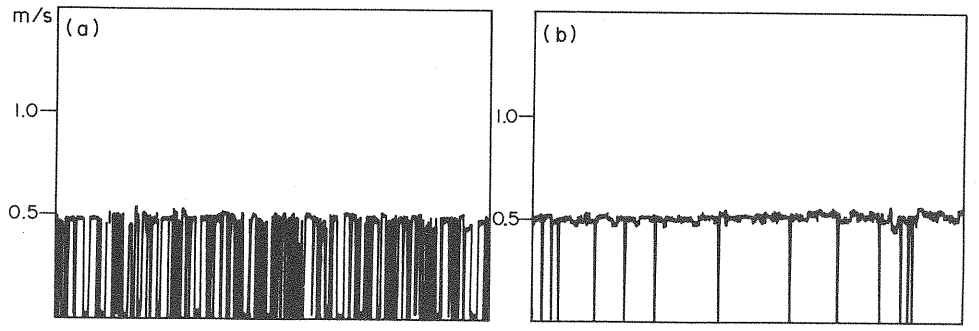

Fig. 9. Recording without any time basis of velocity samples delivered by the counter plus Bragg cell in the two injection patterns 1(a) and 2(b) of the previous experiment.

two phases, as anticipated. Besides, pictures of the flow show that the observed amplitudes of the peaks are in fact equal to the mean rising velocity of the bubbles and hence prove in this particular example the validity of the statements made in Section 3.1 about the experiments conducted in a tank. In this case, the voltage supply seems to be well suited to the measurement of this velocity; but this conclusion has yet to be confirmed when a swarm of bubbles is blown up through the whole test section.

In what follows we shall confine ourselves to the measurement of the parameters characterizing the turbulence in the continuous phase. Accordingly a high voltage supply is used and the typical signal which has to be processed is similar to the one shown in Fig. 10b. Applying a method developed by Delhaye [14] in connection with hot film anemometry, a histogram of the signal amplitude is drawn. In our case, for all experimental conditions investigated this type of histogram is composed of two well defined areas (Fig. 11). As a rule below a critical amplitude $U_c \sim \bar{U}_L^x + 0.2\ \text{ms}^{-1}$ the histogram represents the statistical distribution of the instantaneous velocities within the flow. Beyond the velocities measured are connected to the bubbles signal which in this case is uninteresting, since too noisy. Such velocities have therefore to be suppressed, which can easily be realized with a high amplitude threshold. The error attached to $\bar{U}_L^x$ due to the uncertainty in U_c is then about 1 or 2%. However, we can wonder if this discrimination criterion which can be used here because of the particular form of the velocity histogram still applies to all kind of dispersed two-phase flows. Thus it is clear that it is so, only if the two phases have basically different mean

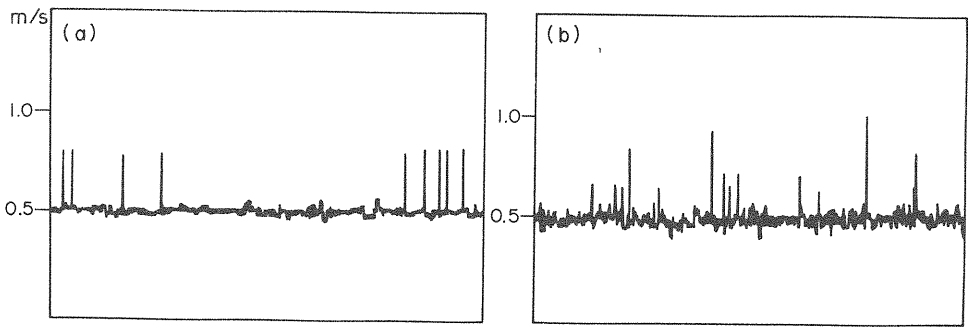

Fig. 10. Two examples of velocity samples recorded without time basis and obtained after the first stage. (a) Air injection located in 3; $\bar{U}_L^x = 0.5\ \text{ms}^{-1}$; low P.M. voltage supply; $\bar{U}_B^x - \bar{U}_L^x = 25$ cm/s. (b) Air injection through the whole test section; $\bar{U}_L^x = 0.5\ \text{ms}^{-1}$; $\alpha = 0.01$ high voltage supply; $\bar{U}_B^x$ undetermined.

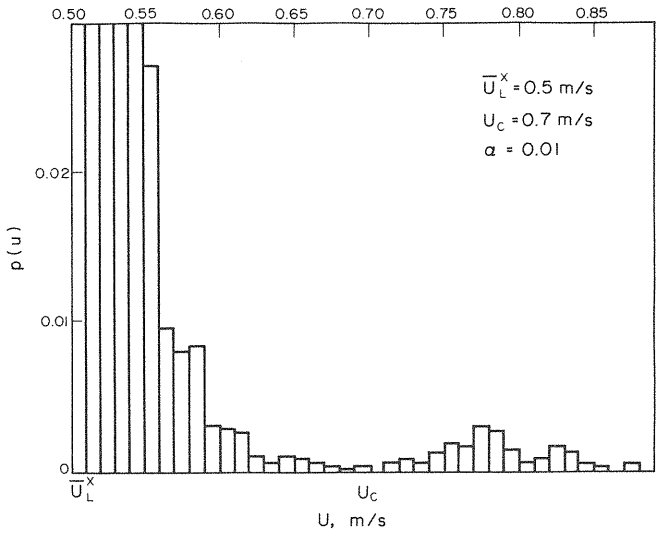

Fig. 11. Histogram of the velocity signal amplitude. Velocities below $\bar{U}_L^x$ are not shown.

velocities. Whenever this condition is not fulfilled, such a discrimination certainly may be difficult or even in extreme cases impossible if the slip velocity becomes nil (e.g. flow of droplets, Lading [15]). But except for such extreme cases it is reasonable to think that the criteria used here can be extended to many other situations.

(c) *Calculation of the turbulence parameters.* The turbulent parameters of the liquid phase are thus evaluated from data for which velocities over $\bar{U}_L^x + 0.2$ ms^{-1} have been eliminated owing to the high amplitude threshold. Averages are made over 10 blocks of 1024 points, which can be considered as a significant statistical sampling as long as the third and fourth order moments of the velocity fluctuations are disregarded. If they are not a minimum of 50 blocks is needed to get an uncertainty in measurement better than 30% (see Section 5). The various moments of the fluctuating velocities of the liquid are calculated by Fortran subprograms using standard algorithms

$$\overline{u_L^2}^x = 1/N \sum_1^N (U_{Li} - \bar{U}_L^x)^2$$

$$S_{uL} = \overline{u_L^3}^x / (\overline{u_L^2}^x)^{3/2} = \sqrt{N} \sum_1^N (U_{Li} - \bar{U}_L^x)^3 \Big/ \left(\sum_1^N (U_{Li} - \bar{U}_L^x)^2 \right)^{3/2}$$

$$T_{uL} = \overline{u_L^4}^x / (\overline{u_L^2}^x)^2 = N \sum_1^N (U_{Li} - \bar{U}_L^x)^4 \Big/ \left(\sum_1^N (U_{Li} - \bar{U}_L^x)^2 \right)^2$$

where U_{Li} stands for the ith validated liquid velocity.

Practically, the low and high amplitude thresholds needed in the signal processing (see 3.2.a and 3.2.b), the Bragg frequency and the fringe spacing are inserted into the main recording program just before the measurements start. This insertion being achieved, the sampled data are then recorded in a few seconds, immediately decoded and the main turbulent parameters are obtained very rapidly: 1 or 2 min for standard parameters, 4–5 min when the components of the Reynolds stress tensor are studied.

4. A CRITICAL EVALUATION OF THE METHOD

In order to test the validity of the method presented in the foregoing paragraphs, Lance's experiments made with a conical hot film [16] were used as a reference and performed all over again, under the same operating conditions. Therefore flows whose mean liquid velocities and local void fractions ranged respectively from 0.4 to 1.2 m/s and from 0 to 3% were investigated. The mean bubble diameter, also kept unchanged was of the order of 5 mm and so, the influence of the bubbles size on the quality of measurements was disregarded. However it seems reasonable to assume that this influence is small and that consequently the conclusions drawn herein are not affected whatever the bubbles size. Finally, the measuring section was approximately located at 31 meshes downstream from the grid which corresponds to a position for which a maximum number of data had been obtained by hot film anemometry. Like Lance, the local void fraction was measured with a waterproof optical probe. The use of this probe as a reference is supported by Galaup's study and the comparisons he made with global measurements based on gamma-ray absorption [17]. The processing system was composed of a Schlumberger counter together with a home-made impulse generator and threshold detector. As regards turbulence intensity levels, we notice on Fig. 12 that the maximum discrepancy between the two methods remains below 10%, i.e. of the same order as the standard uncertainty observed in such measurements, either when using a laser or a hot-film. This holds good for all values of the control parameters, which were investigated [2]. The two types of anemometries may therefore be considered as being in good agreement though the comparison is not so convincing when inspecting the evolution of the higher order moments (third and fourth) of the longitudinal velocity fluctuations (Fig. 13). In fact in the latter case the apparent lack of agreement between the two methods (L.D.A. and H.F.A.) must be attributed to other reasons. It results principally from the limited number of blocks used in the averaging process (see Section 3.2.c). Below 50 blocks the measuring times are of course small (a few minutes as we wished), and the uncertainty attached to such moment measurements is always at least of 20–30% even in single phase flows. On the other hand, a comparatively limited number of reference measurements have been provided by Lance and the sections X/M he investigated are not always the same as that of the present work.

Theoretically the only factor likely to limit the use of a laser in two-phase situations is the mean frequency at which the beams are interrupted. As a matter of fact if the frequency is too high, the measuring times become considerable and thereby make the measurement very difficult or even impossible. The concentration of the dispersed phase for which this occurs, mainly depends on the dimensions of the test section. As a rule it increases when the test section becomes smaller, although it is impossible to predict. For example in the case of an 11 mm dia test section, Ohba and Kishimoto [18] show that laser Doppler anemometry can reasonably be used for all kind of bubbly flows with local void fraction as large as 30%. But in fact this value is also determined by more practical limiting factors of various origins, such as the electronic noise created by the beams interruptions if it cannot be conveniently eliminated, or a too low value of the validated particles ratio. Fortunately, this does not happen here since our method makes it possible to use a high voltage supply of the P.M. and thus to obtain a maximum validation rate, which does not affect the efficiency of the method. With such a voltage, it proves possible to make measurements under void fractions as high as 7% in comparatively limited time intervals (namely a few minutes). It is therefore believed that in our case the critical void fraction ranges from 7 to 10%, perhaps more. Finally it is to be noticed that the L.D.A. is not always well adapted to the measurement of parameters which involve a time sampling, such as one-dimensional energy spectra or time-correlations of the liquid velocity. In fact, the laser validation process being random in time, the classical algorithms commonly employed to calculate the latter quantities become inapplicable.

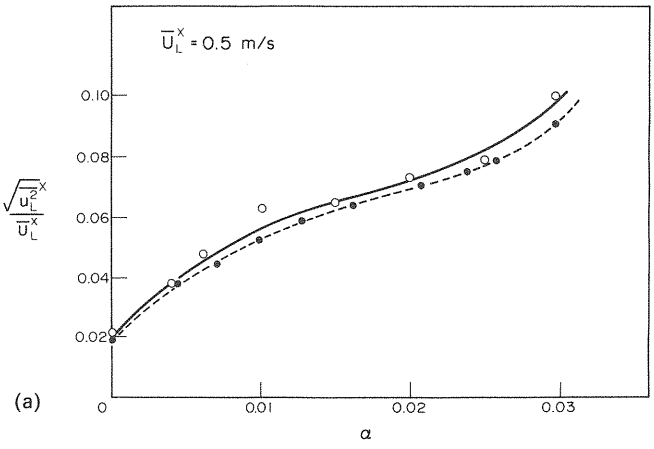

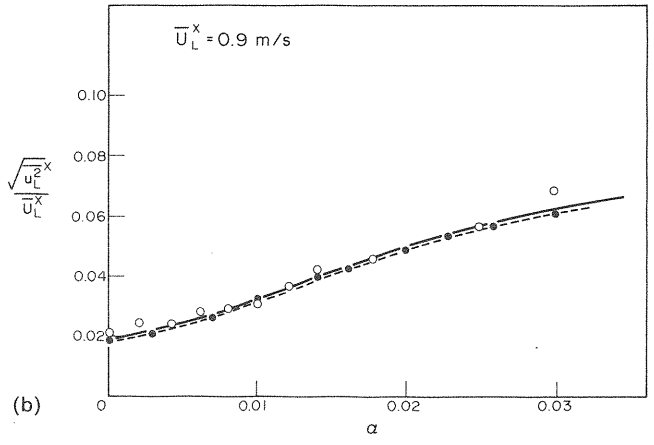

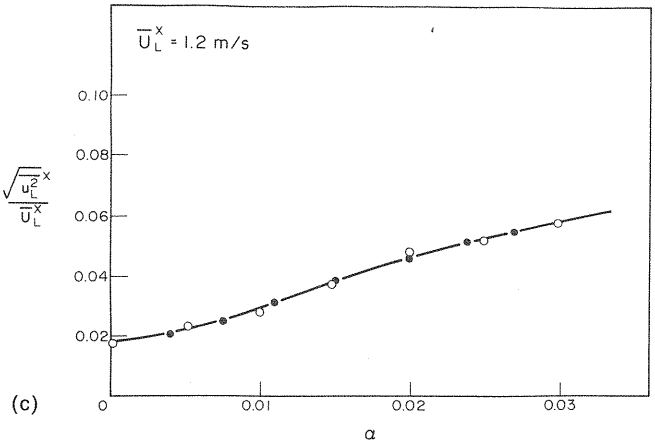

Fig. 12. Evolution of the streamwise turbulent intensity versus local void fraction $\bar{U}_B^x - \bar{U}_L^x \sim 25$ cms^{-1}; ○ laser: $X/M = 31.4$; ● hot-film: $X/M = 31.4$.

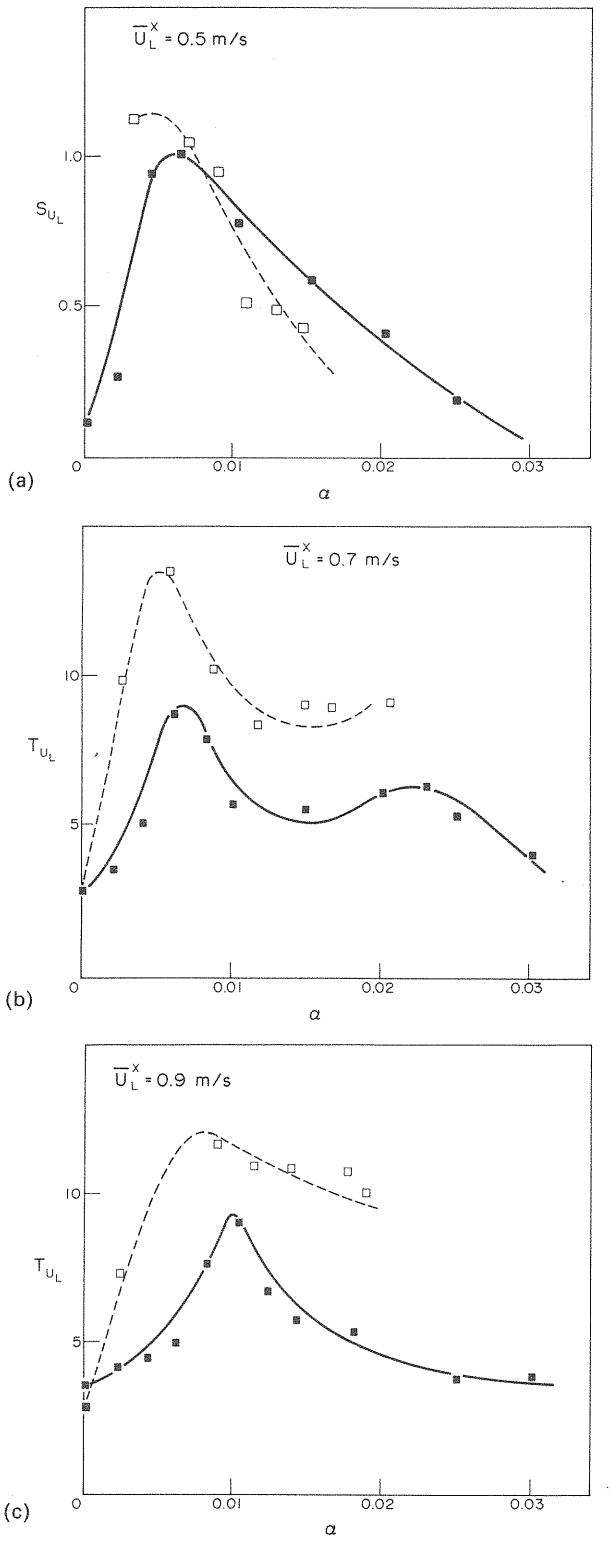

Fig. 13. Evolution of the 3rd (S_{uL}) and 4th (T_{uL}) moment of the longitudinal velocity fluctuations versus local void fraction $\bar{U}_B^x - \bar{U}_L^x \sim 25$ cms^{-1}; ■ laser: $X/M = 31.4$; □ hot-film: $X/M = 36.4$.

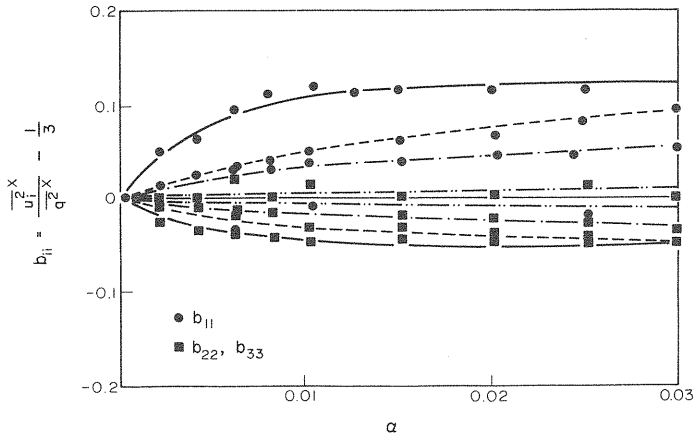

Fig. 14. Components of the Reynolds stress tensor. $X/M = 31.4$.

——— $\bar{U}_L^x = 0$ m/s (liquid initially at rest)
—·—·— $\bar{U}_L^x = 0.5$ m/s
— — — $\bar{U}_L^x = 0.7$ m/s
—··—··— $\bar{U}_L^x = 0.9$ m/s

} $\bar{U}_B^x - \bar{U}_L^x \sim 25$ cms^{-1}.

The present method however, is particularly advantageous when investigating turbulence in a complex two-phase dispersed situation, since no disturbance is created within the flow. Moreover the measurements of the moments of the velocity fluctuations are far easier and much less time consuming than with hot film anemometry, due to the simplicity of the signal processing. For example the Reynolds stress tensor components may be readily secured (see Fig. 14) and the isotropy of the initial turbulence shown to be hardly affected by the presence of bubbles. Finally laser Doppler anemometry provides results which are impossible to obtain otherwise. As an illustration of this last point, the velocity fluctuations generated by the motion of the bubbles in a liquid at rest are given in Fig. 15. It is observed that $\overline{u_L^2}^x$ is proportional to α which confirms the theoretical result found by Theofanous and Sullivan [19].

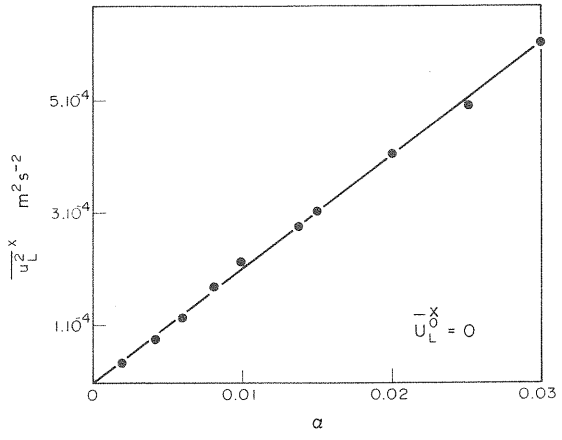

Fig. 15. Velocity fluctuations created by bubble wakes in liquid at rest. $X/M = 3.14$; $\bar{U}_B^x - \bar{U}_L^x \sim 25$ cms^{-1}.

5. CONCLUSIONS

An appropriately modified version of a laser Doppler anemometer has been designed in order to measure the statistical properties of the turbulence of the liquid phase in a bubbly flow, i.e. the various moments of the velocity fluctuations. It is shown that such a technique yields, within limits, results that are in good agreement with those obtained by hot film anemometry and also provides data, such as the Reynolds stress tensor components, which are much more difficult to measure otherwise.

Acknowledgements—The author expresses his deep gratitude to Professor J. Bataille who suggested this study. Special thanks are due to Drs G. Charnay and M. Lance for their numerous and useful comments. The very efficient technical assistance of MM. A. Dumontier and J. P. Melinand is gratefully acknowledged.

The work described in this paper was performed under a C.N.R.S. grant to Ecole Centrale de Lyon.

NOMENCLATURE

χ_L state density function of the liquid phase
$\bar{A}$ statistical average of A
α local void fraction
α_L $= 1-\alpha = \overline{\chi_L}$
A_L parameter relative to the liquid phase
$\bar{A}_L^x$ phase average, $= \dfrac{\overline{\chi_L A_L}}{\alpha_L}$
$\bar{U}_B^x$ mean bubble rising velocity
$\bar{U}_L^x$ mean velocity of the liquid phase in the x direction
u_L fluctuating velocity of the liquid phase in the x direction

REFERENCES

1. F. F. Durst and M. Zaré, Laser Doppler measurements in two-phase flows. SFB 80TM/63, University of Karlsruhe (1975).
2. J. L. Marié, Contribution au développement de l'anémométrie laser à effet Doppler en écoulements diphasiques dispersés. Thèse de Docteur-Ingénieur, Université Lyon I (1981). (Available at CEDOCAR, 26 bd Victor, 75996 Paris Armées, France.)
3. J. M. Delhaye, Two-phase flow instrumentation and laser beam, in *The Accuracy of Flow Measurements by Laser Doppler Methods. Proceedings of the L.D.A. Symposium, Copenhagen* 1975 (Eds P. Buchhave, J. M. Delhaye, F. Durst, W. K. George, K. Refslund and J. H. Whitelaw). Hemisphere, New York (1976).
4. G. F. Hewitt, *Measurement of Two-phase Flow Parameters*. Academic Press, New York (1978).
5. M. Lance, G. Charnay and J. Bataille, A hydrodynamic tunnel for water–air flow turbulence research. *La Houille Blanche* No. 5, 331–335 (1978).
6. A. Boutier, Principe et applications aérodynamiques de la vélocimétrie laser. *Mesures, régulation, automatismes*, 75–87, Avril (1978).
7. F. Durst, A. Melling and J. H. Whitelaw, Laser anemometry; a report on Euromech 36. *J. Fluid Mech.* **56**, part I, 143–160 (1972).
8. W. W. Martin, A. H. Abdelmessih, J. J. Liska and F. Durst, Laser Doppler signal characteristics in particulate two-phase flows. *Int. J. Multiphase Flow*, **7**(4), 439–459 (1981).
9. W. T. Yanta and R. A. Smith, Measurements on turbulence-transport properties with laser-Doppler anemometer. A.I.A.A. Paper 73-169 (1973).
10. K. Ohba, Two phase flow measurements, in *The Proceedings of the Symposium on Long Range and Short Range Optical Velocity Measurements*. pp. XXXV—1–10. I.S.L. (1980).
11. S. L. Lee and J. Srinivasan, An LDA technique for *in situ* simultaneous velocity and size measurement of large spherical particles in a two-phase suspension flow. *Int. J. Multiphase Flow* **8**(1), 47–57 (1982).
12. W. E. R. Davies and J. I. Unger, Velocity measurements in bubbly two-phase flows using laser Doppler anemometry. Parts I & II, University of Toronto, Institute for Aerospace Studies, TN Nos. 184 & 185 (1973).
13. J. P. Sullivan, R. N. Houze, D. E. Buenger and T. G. Theofanous, Turbulence in two-phase flows, in *Transient Two-Phase Flow: Proceedings of the 2nd C.S.N.I. Specialist's Meeting*, 12–14 June 1978. Paris, vol. 2, pp. 583–608. M. Réocreux and G. Katz, Eds, Commissariat à l'Énergie Atomique (1980).

14. J. M. Delhaye, Local measurements in two-phase flow. Fluid Dynamic measurements in the industrial and medical environments, pp. 191–200. (Ed. D. I. Cockrell). Leicester Univ. Press, Leicester (1972).
15. L. Lading, Comparing a laser Doppler anemometer with a laser correlation anemometer, in the *Proceedings of the Conference on the Engineering Uses of Coherent Optics*, University of Strathclyde, Glasgow, pp. 19–36. Cambridge Univ. Press, Cambridge (1975).
16. M. Lance, J. L. Marié, G. Charnay and J. Bataille, Turbulent structure of a co-current air–water bubbly flow, in *Proceedings of the A.N.S./A.S.M.E./N.A.C. International Topical Meeting on Nuclear Reactor-Thermal-Hydraulics "Fundamental Aspects of Two-Phase Flow and Boiling Heat Transfer*, Held at Saratoga Springs, New York, 5–8 October 1980, NUREG/CP-0014, Vol. 2, pp. 1363–1383 (1980).
17. J. P. Galaup, Contribution à l'étude des méthodes de mesure en écoulement diphasique. Applications à l'analyse statîstique des écoulements à bulles. Thèse de Docteur Ingénieur, Université Scientifique et Médicale de Grenoble (1975).
18. K. Ohba, I. Kishimoto and M. Ogasawara, Simultaneous measurement of local liquid velocity and void fraction in bubbly flows using a gas laser. *Tech Rep. Osaka Univ.* **26**(1328), 547–556 (1976).
19. T. G. Theofanous and J. Sullivan, Turbulence in two-phase dispersed flows. *J. Fluid Mech.* **116**, 343–362 (1982).

Communicating Editor: J. M. Delhaye